

See discussions, stats, and author profiles for this publication at: <https://www.researchgate.net/publication/257773916>

# Analysis of Cooperative Behavior in Multiple Kinesins Motor Protein Transport by Varying Structural and Chemical Properties

Article in Cellular and Molecular Bioengineering · March 2013

DOI: 10.1007/s12195-012-0260-9

CITATIONS

13

READS

82

6 authors, including:



**Karthik Uppulury**

Texas Tech University

12 PUBLICATIONS 176 CITATIONS

[SEE PROFILE](#)



**Artem Efremov**

Shenzhen Bay Laboratory

55 PUBLICATIONS 1,531 CITATIONS

[SEE PROFILE](#)



**Anatoly B Kolomeisky**

Rice University

320 PUBLICATIONS 8,129 CITATIONS

[SEE PROFILE](#)

Some of the authors of this publication are also working on these related projects:



Channel Facilitated Molcular Transport [View project](#)



DNA organization by DNA-architectural proteins [View project](#)

# Analysis of Cooperative Behavior in Multiple Kinesins Motor Protein Transport by Varying Structural and Chemical Properties

KARTHIK UPPULURY,<sup>2</sup> ARTEM K. EFREMOV,<sup>1</sup> JONATHAN W. DRIVER,<sup>1</sup> D. KENNETH JAMISON,<sup>1</sup>  
MICHAEL R. DIEHL,<sup>1,2</sup> and ANATOLY B. KOLOMEISKY<sup>2</sup>

<sup>1</sup>Department of Bioengineering, Rice University, Houston, TX 77005, USA; and <sup>2</sup>Department of Chemistry, Rice University, Houston, TX 77005, USA

(Received 31 August 2012; accepted 6 November 2012; published online 21 November 2012)

Associate Editor Jung-Chi Liao & Henry Hess oversaw the review of this article.

**Abstract**—Intracellular transport is a fundamental biological process during which cellular materials are driven by enzymatic molecules called motor proteins. Recent optical trapping experiments and theoretical analysis have uncovered many features of cargo transport by multiple kinesin motor protein molecules under applied loads. These studies suggest that kinesins cooperate negatively under typical transport conditions, although some productive cooperation could be achieved under higher applied loads. However, the microscopic origins of this complex behavior are still not well understood. Using a discrete-state stochastic approach we analyze factors that affect the cooperativity among kinesin motors during cargo transport. Kinesin cooperation is shown to be largely unaffected by the structural and mechanical parameters of a multiple motor complex connected to a cargo, but much more sensitive to biochemical parameters affecting motor–filament affinities. While such behavior suggests the net negative cooperative responses of kinesins will persist across a relatively wide range of cargo types, it is also shown that the rates with which cargo velocities relax in time upon force perturbations are influenced by structural factors that affect the free energies of and load distributions within a multiple kinesin complex. The implications of these later results on transport phenomena where loads change temporally, as in the case of bidirectional transport, are discussed.

**Keywords**—Intracellular transport, Kinesin, Cooperativity.

## INTRODUCTION

Motor proteins are a class of active enzymatic molecules that convert chemical energy of ATP hydrolysis into a mechanical work while transporting cellular materials through highly crowded and viscous environments within cells.<sup>1,9,27</sup> Although the properties of

many microtubule and actin-dependent motors should allow them to perform these functions as single molecules, there are many examples where organelles, vesicles and other sub-cellular commodities are transported simultaneously by teams of motors that function collectively.<sup>4,8,13</sup> In addition, cargos are often outfitted with different types of motors that either move in opposite directions or along different types of cytoskeletal filaments.<sup>15,16,22,24,25</sup> The collective properties of motor proteins are therefore important for understanding mechanisms of intracellular transport because the number of motor proteins, their types and relative numbers of different species might be key factors influencing regulation and control of intracellular processes.<sup>2,3,10,11,18,19,23</sup> Although significant advances in uncovering many features of cellular transport phenomena have been achieved, precise mechanisms of collective action of motor proteins in cells are still not well explained.

Dynamic properties of multiple motor protein assemblies have been investigated in a variety of experimental<sup>2,3,11,18,19,23</sup> and theoretical studies,<sup>5,10,12,14,21</sup> many of which seek to characterize how cargo motion changes with variation in motor number and type. Application of engineered complexes of motor protein has also been very productive in deciphering such responses.<sup>2,3,6,7,10,11,18,19,23</sup> For instance, our group has employed precision particle tracking and optical trapping methods to investigate the dynamic properties of interacting kinesin molecules that are organized on DNA scaffolds.<sup>11,23</sup> As has been found in recent and independent studies that employ antibodies to connect kinesin molecules,<sup>28</sup> these experiments conclude that the functions of complexes containing two kinesins are best characterized as net negative cooperative since the probability of cargo motion by only one load-bearing motor within a complex is generally much

Address correspondence to Anatoly B. Kolomeisky, Department of Chemistry, Rice University, Houston, TX 77005, USA. Electronic mail: diehl@rice.edu, tolya@rice.edu

higher than the probability that both motors will be engaged in transport and cooperate productively. It has also been argued that the weak enhancement of cellular transport in this case is due to high efficiency of single kinesin molecules.<sup>11,14,23</sup>

The above studies of structurally-organized motor complexes have also stimulated significant developments in theoretical analysis of collective behavior of motor proteins.<sup>2,3,10–12,18,19</sup> One of the most successful theoretical approaches is based on a discrete-state stochastic model that captures key elements of single-molecule kinesin dynamics as well as dynamic behavior of two-kinesin assemblies.<sup>5,10,12</sup> This method is unique since it (i) explicitly takes into account individual microscopic transitions between single-motor-bound configurations and a spectrum of two-motor bound configurations with different distances between molecules along filaments; (ii) parameterizes transition rates from fits obtained for single-kinesin optical trap experiments; and (iii) calculates numerically exactly all spatial-temporal dynamic properties of multiple-motor system. This approach reproduces all features observed in experiments on two-kinesin assemblies, and it also provides microscopic explanations for observed dynamic behavior. For example, this model suggests that collections of kinesins face mechanical and kinetic challenges that restrict their ability to adopt filament-bound configurations that support load-sharing behaviors. Furthermore, discrete state modeling has also demonstrated that this behavior is only exacerbated when applied loads vary spatially and temporally.<sup>10</sup> Yet, such behaviors naturally raise fundamental questions as to whether such dynamics is general for all motor proteins or it is unique for structurally organized kinesin complexes utilized in our experiments. Herein, we apply the discrete-state stochastic modeling approach to examine the extent to which multiple

kinesin behaviors change with varying structural and chemical properties of a multiple motor system.

## METHODS

Our analysis of motor protein cooperativity is based on a discrete-state stochastic approach that has been developed to explain optical trapping measurements obtained for two-kinesin assemblies acting on cargos against applied external loads.<sup>6,7,26</sup> A generic view of the system of two kinesins that move cargo is shown in Fig. 1(Left). It is assumed that two kinesins are bound at a distance  $S_{\text{bead}}$  apart from each other on the surface of a spherical cargo with a diameter  $D$ . The motors can attach and detach to and from different microtubule lattice sites that are separated by 8.2 nm, and they are assumed to move only along a single protofilament for simplicity. The model enumerates for a broad range of transitions where only one motor protein molecule is connected to microtubules as well as a wide spectrum of two-motor-bound configurations where the separation distance between binding sites on microtubules,  $S_{\text{microtubule}}$ , varies.

### Transition Rate Modeling

The main idea of the discrete state stochastic approach is to calculate the rates a multiple motor complex transitions between different filament-bound configurations *via* explicit calculations of the free energy of the system in each state. It is done by assuming that between transitions the system quickly relaxes to mechanical equilibrium, although chemical equilibrium is not assumed.<sup>6,7,26</sup> The forces acting on the cargo and the motors are estimated from the force-balance assumption and parameterizing the stiffness

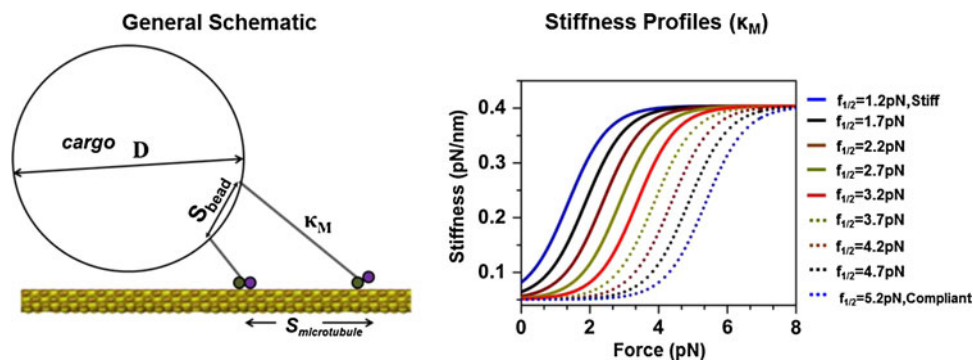


**FIGURE 1.** (Left) A schematic representation of the model of cargo transport by two coupled kinesin motor proteins along the microtubule. The cargo diameter is  $D$ , the separation distance between the motors on the cargo surface is  $S_{\text{bead}}$  and that on the microtubules is  $S_{\text{microtubule}}$ . (Right) Plots of motor stiffness ( $\kappa_M$ ) that show the strain-induced stiffening of a single kinesin-bead linkage under load. The legend indicates the force at which motor stiffness reaches half of its maximal value ( $f_{1/2}$ ). The red curve ( $f_{1/2} = 3.2$  pN) approximates the stiffness function of the kinesin motors examined experimentally in Rogers *et al.*,<sup>23</sup> Jamison *et al.*<sup>11,10</sup>

profile of the kinesin motor from experiments. The free energy of the complex, which is called a configurational energy ( $E_{\text{config}}$ ), can then be calculated explicitly using the following expression:

$$E_{\text{config}} = \frac{1}{2}k_{\text{T}}(x_{\text{T}} - x_{\text{b}})^2 + \sum_{\text{M}} \int_{l_0}^{l_{\text{ax}}} \|\vec{F}_{\text{ax}}\| dl \quad (1)$$

where,  $k_{\text{T}}$ ,  $x_{\text{T}}$ ,  $x_{\text{b}}$  and  $F_{\text{ax}}$  are the trap stiffness, position of the trap, position of the cargo bead center and the axial load experienced by the bead respectively. The parameter  $l_0$  denotes the length of the kinesin motor under zero force, while the parameter  $l_{\text{ax}}$  is the extended length of the motor protein. This equation reflects two contributions into the free energy of the state, the potential energy of the bead in the trap and the mechanical energy associated with stretching the motor protein—see Driver *et al.*<sup>6</sup> for more detailed explanations.

The way the system of coupled motor proteins evolves with a time is given by a set of master equations that are numerically solved as explained in detail in our previous works.<sup>6,7,26</sup> The calculated free energies are utilized for estimating transition rates *via* the detailed balance conditions. Solving master equations provides probability distributions of different states of the system at various times, which can be used to estimate average observable quantities such as average detachment rates, detachment forces and cargo velocities that, in turn, can be used to assess whether the motors within a complex can cooperate productively.

### Model Parameterization and Calculating Observables

Transition rates are input parameters for solving master equations, and they are obtained in the following way. Detachment and binding rates in the absence of external forces are estimated from experimental analyses of single kinesin behaviors exclusively,<sup>7,26</sup> and the rates under loads are determined using the detailed balance condition as explained in Driver *et al.*<sup>6</sup> Stepping rates of the motor under applied loads are determined from fits to single-kinesin optical trapping data: see Driver *et al.*<sup>6</sup> for more details. To properly describe mechanical properties of the system, the elasticity of motor–cargo links is estimated by using fits to measurements of single-kinesin stiffnesses.<sup>7,11</sup> These results show the non-linear elasticity of the system which allows us to take into account the effects of strain-induced stiffening of connections between motor proteins and cargo.

The present analyses examine how collective kinesin behaviors change with structural and mechanical properties of a multiple motor complex as well as biochemical properties of its constituent motors. Our

prior experiments utilized a DNA scaffold that separated the motors by 50 nm on surface of 500 nm sized beads.<sup>10,11</sup> For the present study, the influence of a motor complex’s structure was examined by altering the distance between motor protein connections on the bead  $S_{\text{bead}}$  and cargo size  $D$ . The effect of mechanical properties was also explored by varying elastic properties of motor protein complexes. Again, experimental measurements of force-dependent elasticity of single kinesins<sup>6,11</sup> indicate that the motor protein stiffness has a non-linear dependence due to strain-induced stiffening of the motors (Fig. 1). We have shown that these responses can be approximated well by a sigmoid function.<sup>6,11</sup> To simplify the present analyses, our original function was modified by altering the force at which motor stiffness increase with increasing load. To label different load-dependent stiffness curves we introduce a quantity  $f_{1/2}$ , which corresponds to the force at which motor stiffness ( $\kappa_{\text{M}}$ ) reaches half of its maximal value. Accordingly, high  $f_{1/2}$  corresponds to more compliant motors, while smaller values describe rigid motor proteins. Experimental measurements of elasticity for kinesins give  $f_{1/2} = 3.2 \text{ pN nm}^{-1}$ .<sup>11</sup> Then for each elasticity behavior specified by different curves (Fig. 1Right) dynamic properties of the system are evaluated directly and compared with each other to quantify the effect of motor protein stiffness on cooperativity.

The effect of chemical interactions between kinesins and microtubules can be taken into account by modifying detachment forces and detachment rates. Such effects can be explored by modulating the unloaded rate for single motor detachment ( $\varepsilon$ ). We also define and modulate kinesin’s critical detachment force ( $F_{\text{d}}$ ), which is the characteristic force that exponentially decreases the rate of motor protein dissociation from the microtubule. The critical detachment force is also associated with the length scale  $L_{\text{d}}$ , *via*  $F_{\text{d}} = kT/L_{\text{d}}$ , that describes the distance needed to move the motor protein molecule away from the microtubule to be considered detached. The structurally-defined kinesin complexes described in Driver *et al.*<sup>6</sup> can be modeled using the experimentally determined values of  $\varepsilon = 0.312 \text{ s}^{-1}$  and  $F_{\text{d}} = 3.1 \text{ pN}$ . For simplicity, we assume that motor detachment follows Kramer’s-type dependence, although experimental data are better described by a two-state model.<sup>6</sup> We utilize this approach to simplify all computations, since experimentally observed trends are not affected by this approximation and only some small quantitative features are changed. It is important to note that, in contrast to some treatments, we have shown that this approximation can still lead to average detachment rates for multi-motor complexes that are not exponential functions of forces. Thus, we predict multiple

motor behaviors that exhibit apparent deviations from Bell-model predictions without the need to assume that motors exhibit complex, force-dependent detachment characteristics such as slip–catch behaviors.<sup>6</sup>

To quantify the influence of all these structural, mechanical and chemical properties, we concentrate on several observable quantities that are measured in experiments and that can be easily calculated in the discrete-state approach. Specifically, in this work, we calculate the free energy difference,  $\Delta E_{\text{config}}$ , between single-bound and a range of two-motor states since motor protein molecules can only cooperate productively when they are bound close together to the microtubule. Similarly, one could see the effect of cooperativity by monitoring the ratio of average detachment forces for two-motor bound and single-motor bound cargo complexes,  $\langle F_2 \rangle / \langle F_1 \rangle$ . A dynamic view of cooperativity can also be obtained from analysis of the ratio of average velocities for two-motor and single-motor complexes,  $\langle V_2 \rangle / \langle V_1 \rangle$ .

Recent force clamp assays have shown that multiple kinesin complexes may experience loading conditions that prevent them from reaching a steady state; for example, when loads vary spatially or temporally.<sup>6</sup> Consequently, understanding mechanisms of motor cooperation also requires analyses of the relaxation behavior of motor protein complexes under variable loading conditions. Generally, if the applied load is changed instantaneously from a low to high load, multiple kinesin velocities will also change in time as the system progresses towards a new steady state since the probability that a complex will achieve productive, load-sharing states increases with increasing load. The characteristic relaxation time describing this change can be approximated using the following exponential function:

$$V_{\text{av}}(t) = A - B \exp\left(-\frac{t}{\tau_{\text{relax}}}\right) \quad (2)$$

In this expression, the parameter  $A$  corresponds to a stationary-state velocity, while the parameter  $B$  gives the deviation from the stationary-state velocity at

initial times. The values of  $A$ ,  $B$  and  $\tau_{\text{relax}}$  are extracted from fits to calculated curves.

Relaxation times were calculated for a circumstance where the applied load increased instantaneously from 4 to 5 pN, and then remained static at 5 pN until the system reached its steady state. This condition mimics those provided in our prior force clamping assays.<sup>6</sup> A complete set of parameters used in our calculations is presented in Table 1.

## RESULTS AND DISCUSSIONS

As discussed in Driver *et al.*<sup>11</sup>, the distribution of an applied load between two elastically-coupled kinesins when both motors are attached to a microtubule is strongly dependent on how far apart the motors are bound at the filament. Due to geometric constraints, equitable load sharing only occurs when the motors are bound closely on the filament, and hence, they will only cooperate productively under an applied load if they can transition into these states. To gauge how structural and mechanical properties of a complex influence this ability, we first examined dependence of configurational energy changes of a two-kinesin complex on cargo diameter ( $D$ ), the distance between the sites that the motors are anchored to the cargo surface ( $S_{\text{bead}}$ ), and the mechanical compliances of motor–cargo linkages (*via* the parameter  $f_{1/2}$ ). In each case, configurational energies were calculated for transitions from single-motor bound states to a range of two-motor bound configurations. Generally, the lower this energy difference the higher the degree of cooperativity since the system will transition more frequently into two-motor bound states where the motors will share their load (see Figs. 2, 3), and since transition probabilities will be controlled by the corresponding Boltzmann’s factor:  $\exp(-\Delta E_{\text{config}}/k_{\text{B}}T)$ .

The dependence of  $\Delta E_{\text{config}}$  for different sized cargos as a function of the separation distance between the motors on the microtubule are presented for applied

**TABLE 1. Model parameters and their estimated values.**

Parameter	Estimated/measured values	Reference
$\pi_0$ unloaded binding rate	$4.7 \text{ s}^{-1}$	Estimated from Leduc <i>et al.</i> <sup>17</sup>
$\varepsilon_0$ unload detachment	$0.312 \text{ s}^{-1}$	Estimated from Driver <i>et al.</i> <sup>6</sup>
$u_{++}^0$ , unloaded stepping rate	$1.59 \times 10^{14} \text{ s}^{-1}$	Estimated from Driver <i>et al.</i> <sup>6</sup>
$u_{+-}^0$ , unloaded stepping rate	$61.7 \text{ s}^{-1}$	Estimated from Driver <i>et al.</i> <sup>6</sup>
$w_{-}^0$ , unloaded stepping rate	$0.654 \text{ s}^{-1}$	Estimated from Driver <i>et al.</i> <sup>6</sup>
$w_{+-}^0$ unloaded stepping rate	$1.69 \times 10^9 \text{ s}^{-1}$	Estimated from Driver <i>et al.</i> <sup>6</sup>
$F_{\text{d}}$ , detachment force	3.1 pN	
$D$ , cargo diameter	300–700 nm	See text for details
$S_{\text{bead}}$ separation distance	30–70 nm	See text for details
$f_{1/2}$ stiffness at half-maximum	1.2–5.2 pN	See text for details

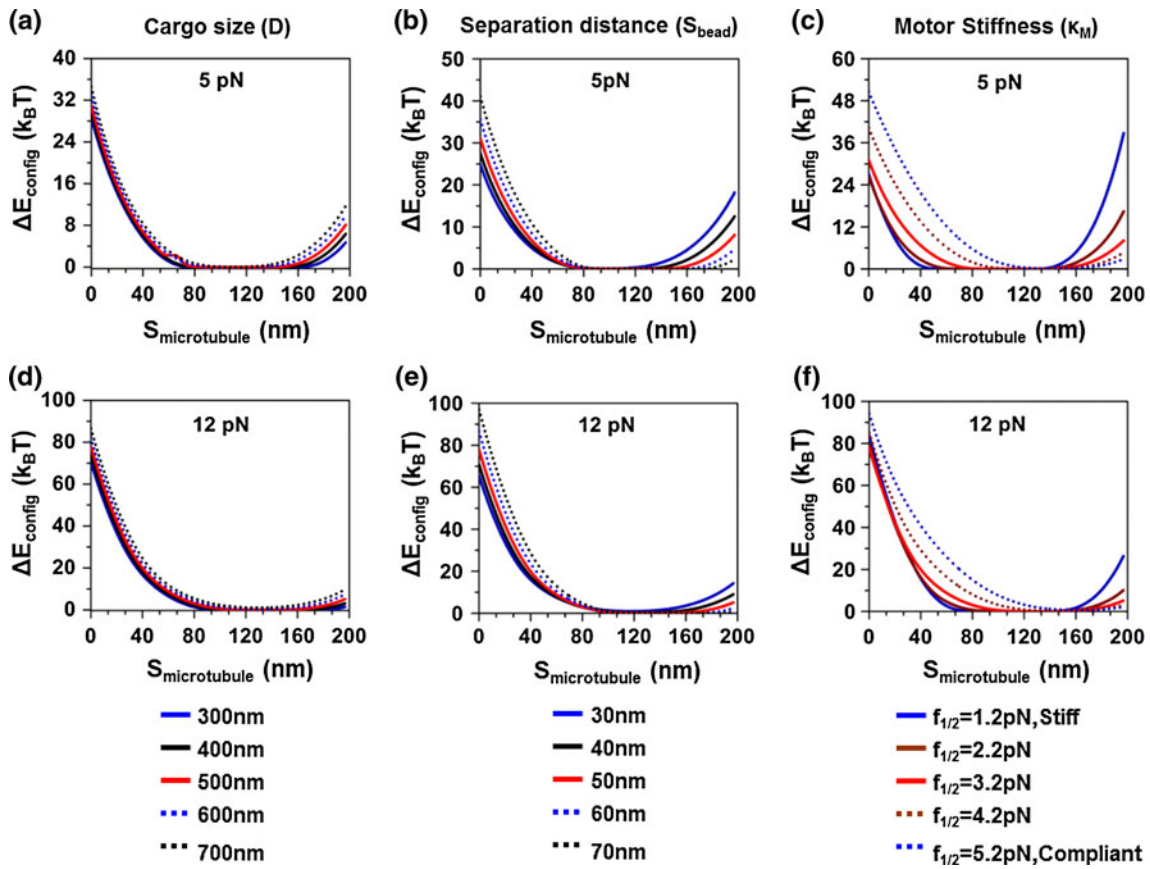


FIGURE 2. Difference in configurational energies between two-motor and single-motor states as a function of structural and chemical parameters. (a)  $\Delta E_{\text{config}}$  for varying cargo diameter ( $D$ ) at 5 pN applied load. (b)  $\Delta E_{\text{config}}$  for varying separation distances ( $S_{\text{bead}}$ ) at 5 pN. (c)  $\Delta E_{\text{config}}$  for varying motor stiffness at 5 pN load. (d)  $\Delta E_{\text{config}}$  for varying cargo diameter ( $D$ ) at a 12 pN load. (e)  $\Delta E_{\text{config}}$  for varying separation distances ( $S_{\text{bead}}$ ) at a 12 pN load. (f)  $\Delta E_{\text{config}}$  for varying motor stiffness at a 12 pN load.

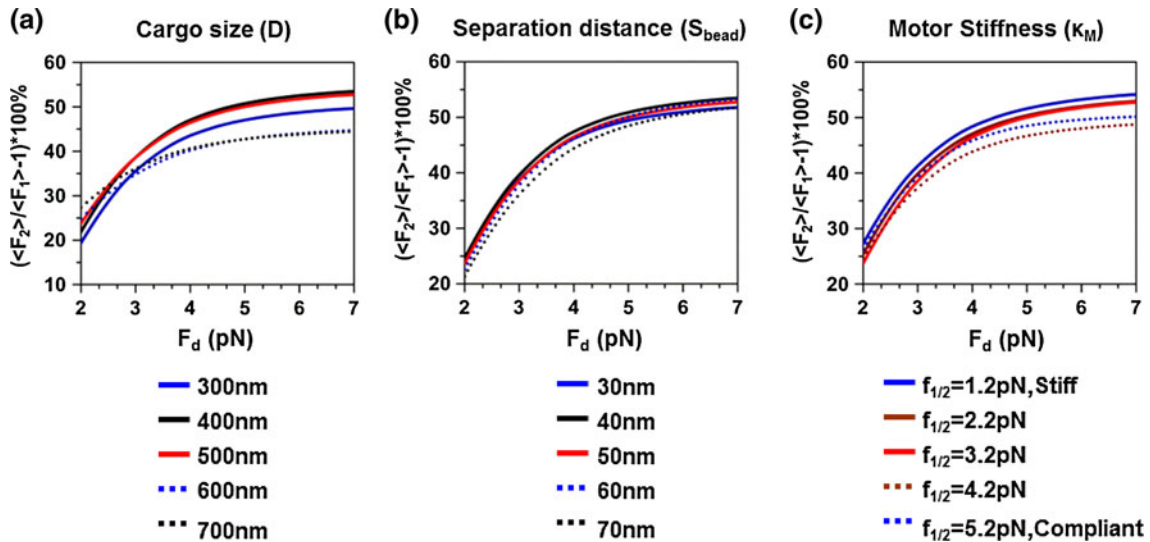


FIGURE 3. Analyses of increases of cargo detachment forces due to motor cooperation. The percentage increase  $(\langle F_2 \rangle / \langle F_1 \rangle - 1) * 100\%$  is computed in the panels a, b and c correspond to the cases of varying cargo diameter ( $D$ ), separation distance ( $S_{\text{bead}}$ ) and motor stiffness ( $\kappa_M$ ).  $\langle F_2 \rangle$  is the average detachment force compiled from the detachment force distribution of a two-motor cargo complex while  $\langle F_1 \rangle$  corresponds to that of a single-motor molecule.

loads of 5 pN in Fig. 2a, and for 12 pN in Fig. 2d. The results of each calculation shows there is a relatively large range of intermediate  $S_{\text{microtubule}}$  values where  $\Delta E_{\text{config}}$  is negligible since transitions into these configurations do not change the force balance between the motors in a complex. Outside of this region,  $\Delta E_{\text{config}}$  changes more rapidly with  $S_{\text{microtubule}}$  compared to the cargo size  $D$ . Although the effects are very small, the energy needed to transition into configurations where the motors are closely spaced on the microtubule is found to increase with the increasing cargo size (Figs. 2a, 2d). Moreover,  $\Delta E_{\text{config}}$  is found to be sensitive to cargo size for transitions into states where the motors are positioned far apart on the filament ( $S_{\text{microtubule}} > 140$  nm) and will experience additional ‘counter forces’ due to the resultant leading–lagging–motor organization of the complex in these configurations.<sup>11</sup> Nevertheless, given the magnitude of these differences, we generally expect that cargo size will not affect the probabilities the motors will share their loads appreciably.

While also small compared to the dependence of  $\Delta E_{\text{config}}$  on  $S_{\text{microtubule}}$ , somewhat stronger dependences of  $\Delta E_{\text{config}}$  are predicted when the separation distance between the motors on the bead ( $S_{\text{bead}}$ ) is increased (Fig. 2b—for 5 pN; and Fig. 2e—for 12 pN). These trends can be understood from the system geometry (Fig. 1Left). When  $S_{\text{microtubule}} < 100$  nm, increasing the cargo diameter  $D$  or  $S_{\text{bead}}$  makes it harder for the second motor to bind to the microtubule because the motors must now stretch a larger distance to reach their corresponding lattice sites, which is more energetically costly. It is also important to note that the free energy of the system could be further affected by bead rotations and displacements against the applied load, as discussed in Driver *et al.*<sup>6</sup> Note also that for  $S_{\text{microtubule}} > 100$  nm,  $\Delta E_{\text{config}}$  decreases with increasing  $S_{\text{bead}}$ , in contrast to the dependence on cargo diameter  $D$ . Although neither structural parameter is shown to influence  $\Delta E_{\text{config}}$  significantly compared to the on-filament motor spacing, this distinction occurs since the vectorial properties of the loads experienced by each motor (i.e., the split between tangential and upward loads on a motor) will change differently when cargo size and motor spacing are varied—due to bead curvature.

The elasticity of motor proteins in a motor-bead linkage is predicted to have the strongest effect on the free energy difference between two-motor and single-motor bound states (Figs. 2c, 2f). This response can be explained as follows. Under the same external load ( $F$ ), the cargo displacement is given by  $\Delta x = F/\kappa_M$ , which leads to the free-energy contribution of  $\frac{1}{2} \kappa_M \Delta x^2 = 1/2 F^2/\kappa_M$ . This result states that increasing the stiffness lowers the contribution to free energy. This simple argument therefore predicts that more rigid

motors should cooperate better since they do not increase  $E_{\text{config}}$  as much as do the more compliant motors. These arguments work well for  $S_{\text{microtubule}} < 100$  nm. However, the trend reverses for larger separation distances due to the introduction of counter forces which increase load per each motor molecule (see Fig. S3 in Driver *et al.*<sup>6</sup>). Yet, we expect the dependence of  $E_{\text{config}}$  on  $\kappa_M$  to mimic the trend found with  $S_{\text{bead}}$ , as opposed to the trend for cargo diameter  $D$ , since compliant motors can stretch more easily. A more flexible complex will therefore behave effectively as motors that are spaced further apart on the bead when they adopt configurations where  $S_{\text{microtubule}}$  is large.

A different way of analyzing cooperativity of multiple motor proteins is to compare average detachment forces of two-motor complexes ( $\langle F_2 \rangle$ ) and single-motor molecules ( $\langle F_1 \rangle$ ). These forces can be determined from detachment distributions obtained in the static trap mode of experiments.<sup>11</sup> If two-motor assemblies cooperate positively *via* load sharing, it will take much more energy to remove them from the microtubules. But if the cooperation is weak the detachment force  $\langle F_2 \rangle$  for two motor protein molecules should not be significantly larger than the detachment force  $\langle F_1 \rangle$  for the single-motor case. It is important to note that we are considering here the detachment force rather than the stalling force which only describes the condition of no motion for the cargo without providing microscopic details on mechanisms of cooperativity.

The percentage increase  $(\langle F_2 \rangle / \langle F_1 \rangle - 1) * 100\%$  as a function of the cargo size, geometry and motor stiffness is shown in Fig. 3 and are plotted as a function of the critical detachment forces  $F_d$ , which is a force that characterizes the sensitivity of motor detachment to strain.<sup>6,7</sup> Increasing the cargo diameter lowers the ratio  $\langle F_2 \rangle / \langle F_1 \rangle$  as expected (Fig. 3a) since in this case it becomes easier energetically to detach two-motor complexes, leading to lower cooperativity. Similar effect is observed for increasing the distance between bound motors (Fig. 3b), although the effect is smaller. In addition, more rigid motors also increase the cooperativity with respect to force production (Fig. 3c); in agreement with our free-energy arguments. *Nevertheless, one can clearly see that the  $\langle F_2 \rangle / \langle F_1 \rangle$  ratio for all ranges of reasonable parameters is only slightly larger than 1, indicating weak cooperative gains and a generic insensitivity to a multiple motor system’s structural and mechanical properties.* The largest gains and dependencies on the structural and mechanical properties of the complex are observed when  $F_d$  is assumed to be very large (6–7 pN) which most probably are not realistic for typical cellular conditions. This is due to the fact that larger  $F_d$  corresponds to stronger interactions between motor

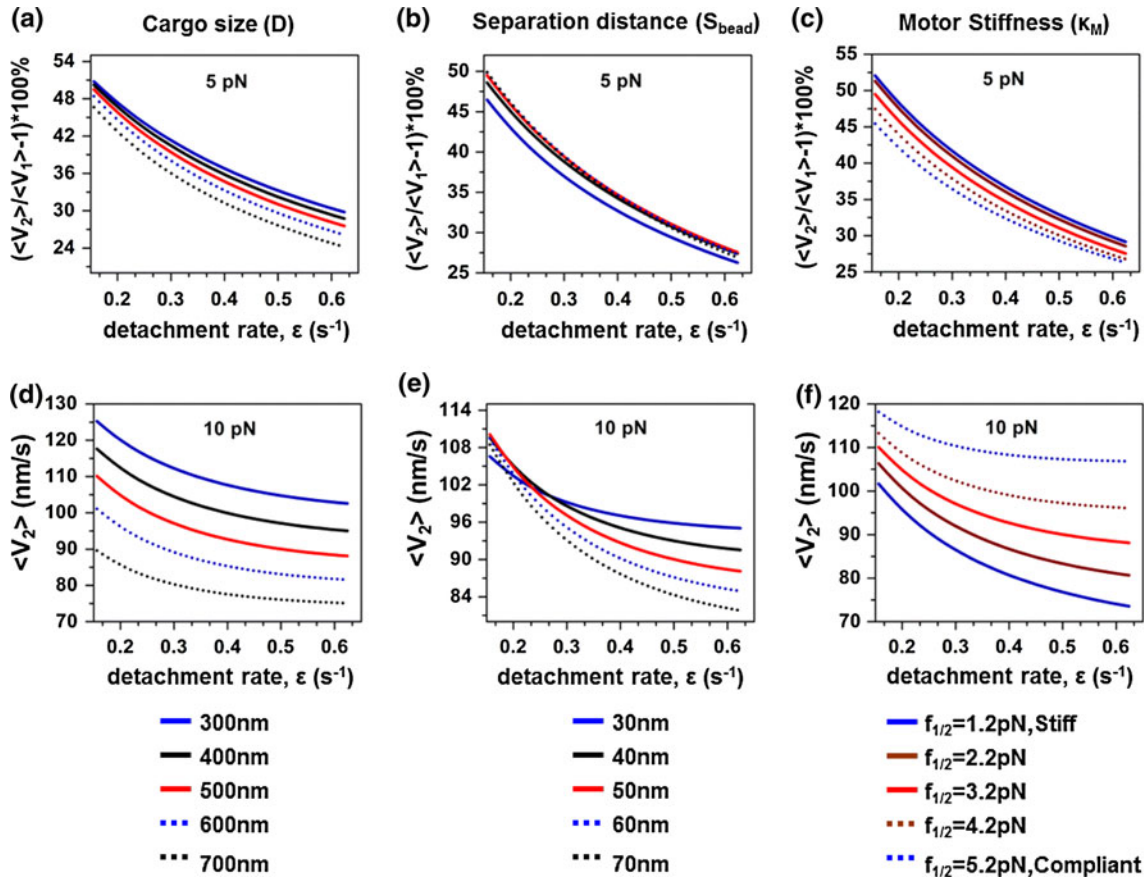


**FIGURE 4.** Responses of multiple motor velocities to changing structural, mechanical and biochemical parameters. Steady-state cargo velocities of a two kinesin complex are denoted as  $\langle V_2 \rangle$  and that of a single kinesin-1 complex is  $\langle V_1 \rangle$ . (a) The function  $(\langle V_2 \rangle / \langle V_1 \rangle - 1) * 100\%$  at 5 pN for varying cargo size ( $D$ ). (b) The function  $(\langle V_2 \rangle / \langle V_1 \rangle - 1) * 100\%$  at 5 pN for varying  $S_{\text{bead}}$ . (c) The function  $(\langle V_2 \rangle / \langle V_1 \rangle - 1) * 100\%$  at 5 pN for varying motor stiffness ( $\kappa_M$ ). (d)  $\langle V_2 \rangle$  at 10 pN for varying cargo size. (e)  $\langle V_2 \rangle$  at 10 pN for varying  $S_{\text{bead}}$ . (f)  $\langle V_2 \rangle$  at 10 pN for varying motor stiffness.

proteins and microtubules, and it leads to longer lifetimes of two-motor complexes under load, yielding higher probability for cooperative interactions with load sharing.

Another convenient measure of cooperative effects is the average cargo velocities driven by two-motor complexes  $\langle V_2 \rangle$  compared to average cargo velocities produced by single motor molecules  $\langle V_1 \rangle$ . The expectation is that when motors cooperate positively under an applied load,  $\langle V_2 \rangle$  is significantly larger than  $\langle V_1 \rangle$ . For these analyses, we calculated steady-state cargo velocities for force-clamp conditions where the external load is held constant.<sup>6</sup> The percentage increase  $(\langle V_2 \rangle / \langle V_1 \rangle - 1) * 100\%$  is presented in Figs. 4a–4c for an applied load of 5 pN, and it is presented as a function of a motor's unloaded detachment rate ( $\epsilon$ ) for several motor systems where the cargo diameter  $D$ ,  $S_{\text{bead}}$  and  $\kappa_M$  are varied. We chose to employ force-clamp conditions and to modulate motor detachment rates since this approach allows us to best isolate the dependence of cargo velocities on the strength of a motor's interaction with

the microtubule filament (e.g., spatial and temporal effects can be neglected). Single kinesin will stall at loads exceeding 7 pN, yielding aberrantly-high ratios  $\langle V_2 \rangle / \langle V_1 \rangle$  ratios. For this reason, we present in Figs. 4d–4f absolute values of cargo velocity when it is driven by the motor-protein complex for the external load of 10 pN.

The response of multiple kinesin velocities to structural/geometric and mechanical parameters is presented in Fig. 4. As is found for detachment forces, differences between single and two-kinesin velocities are exceptionally small ( $< 2\%$  for nearly any value of  $\epsilon$ ) when the applied load is small ( $F = 5$  pN). More significant differences are found at high applied loads ( $F = 10$  pN). The latter response can be explained by the fact that cargos will stall when only one of the complex's motors is engaged in transport, producing very large differences in cargo velocities when the system is bound in these states compared to load-sharing states. Cargo velocities will therefore be very sensitive to alterations in the probability that the system will enter into either of these classes of states.



The dependence of multiple kinesin velocities on the structural and mechanical properties of a complex generally follows the trends found with cargo detachment forces; again, these changes are negligible when applied loads are small (Figs. 4a–4c). The only exception is found with motor stiffness. Increased motor compliance (increasing  $f_{1/2}$ ) produces lower cargo velocities when applied loads are below kinesin’s stalling force (Fig. 4c). However, this trend is reversed at large loads (Fig. 4f). We believe that this behavior stems from the fact that the compliant motors will stretch very large distances under these loads. Such behavior therefore increases the range of motor bound configurations where the motors will share their load equitably; hence, allowing the motors to step more rapidly compared to those in a rigid complex that is bound in similar configurations (this effect is illustrated in Fig. S3 in Jamison *et al.*<sup>11</sup>). This response therefore illustrates the importance of analyzing the vectorial properties of load distributions within multiple motor complexes when assessing cooperative effects. Nevertheless, it is also important to recognize that the low average detachment forces produced by compliant motor complexes will reduce the probability that a cargo will be transported to such loads. Thus, despite the trend found in Fig. 4f, the weak cooperative behaviors found in those analyses will likely dominate multiple kinesin behaviors.

As was found with the dependence of multiple motor detachment forces on  $F_d$ , our calculations show that motor cooperativity is generally much more sensitive to biochemical factors affecting motor affinity than the structural and mechanical properties of the complexes, especially at small applied loads. For example, significant changes to two-motor velocities are predicted when the unloaded detachment rate of a

single motor molecule ( $\varepsilon$ ) is varied (Fig. 4). This can be understood in the following way. Decreasing the detachment rate increases the time that motors spend bound to microtubules; thus, increasing the probability a complex will generate high-velocity and cooperative load-sharing states. At the same time, cooperativity is reduced for large detachment rates since the motors will detach before these states are reached. Given the strong sensitivity of multiple kinesin velocities to  $\varepsilon$ , we conclude that factors influencing how tightly the basal affinity of motors to their filaments as well as the sensitivity of motor–microtubule interactions to load will influence multiple kinesin behaviors more significantly than the structural and mechanical properties of the complexes, which primarily determine how load is distributed within a complex.

Finally, we also examined how the multiple kinesin velocities change in time by examining how fast cargo velocities relax to a steady-state velocity after an instantaneous change in the applied load. Although neglected in many multiple motor analyses, understanding such behavior is important since these relaxation times will influence whether a multiple motor system will achieve a steady-state during transport scenarios where applied loads vary temporally. Relaxation occurs since the distributions of multiple motor-bound configurations depend on the applied load on a cargo. Relaxation rates/times will naturally depend on how complexes transition between different configurations in time *via* motor binding, detachment and stepping. To analyze this behavior, we calculated relaxation times by starting computations of the two-kinesin system at applied load  $F_{ap,0}$  and changing it to another applied load  $F_{ap,1}$ . The data presented in Fig. 5 corresponds to case where the load was jumped from 4 to

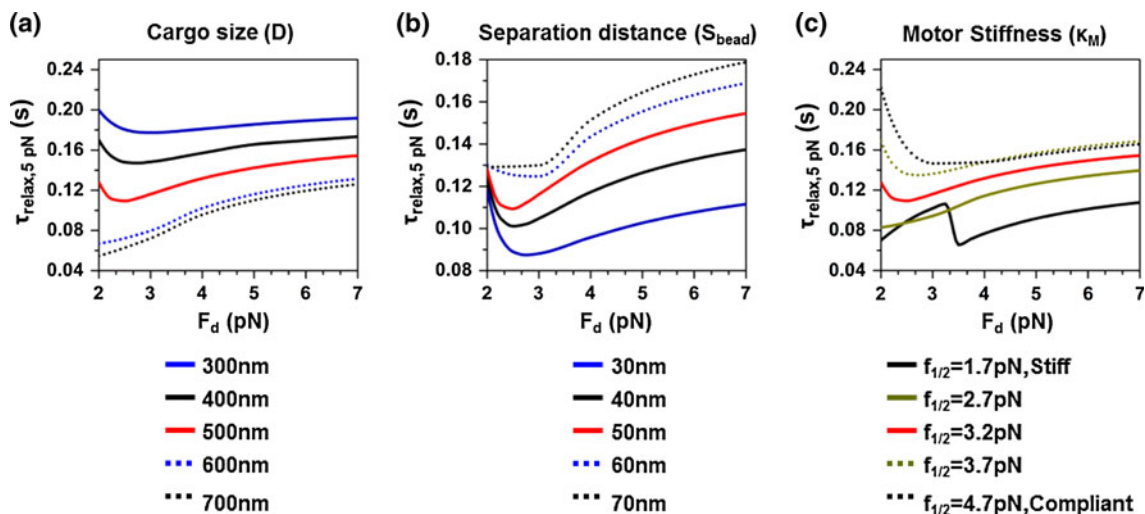


FIGURE 5. The relaxation time ( $\tau_{relax}$ ) for different structural, mechanical and chemical properties. (a)  $\tau_{relax}$  at 5 pN applied load for varying cargo sizes ( $D$ ). (b)  $\tau_{relax}$  at 5 pN for varying separation distances ( $S_{bead}$ ). (c)  $\tau_{relax}$  at 5 pN for varying motor stiffness  $\kappa_M$ .

5 pN, but as we checked to confirm that qualitative results are not strongly dependent on the magnitude of these changes in load. Relaxation times were determined using the procedures described in the “Methods” section.

The dependence of relaxation times on different structural properties of the system is shown in Fig. 5. Interestingly, in contrast to multiple kinesin detachment forces and velocities, relaxation times are found to exhibit strong dependencies on the structural and mechanical properties of a cargo. While the evolution of motor-complexes bound geometry is a complex process involving motor binding detachment and stepping, we believe that there are some general features of relaxation dynamics that can be understood by analyzing the configuration-dependent free energies of the complexes. For example, relaxation times decrease for larger cargo sizes (Fig. 5a). The analyses of  $\Delta E_{\text{config}}$  in Fig. 2a show that the range of states where the energetic costs associated with transitions from single- to two-motor bound configurations are negligible also decreases as cargo diameter ( $D$ ) increases. Consequently, the number of states occupied by a motor complex on a large cargo will likely decrease with increasing the cargo size, yielding smaller relaxation times. Multiple kinesin velocities also relax faster when  $S_{\text{bead}}$  is small (Fig. 5b) and when their linkages to the beads are stiff (Fig. 5c). These responses may seem to contradict the trend found with cargo size. However, closer examination show of the states at large motor separation distances (Figs. 2b, 2c) as well as load distributions (Fig. S3 in Jamison *et al.*<sup>11</sup>) uncovers similar effects. In these cases, the range of ‘energetically neutral’ states decreases as  $S_{\text{bead}}$  and motor compliances increase. Furthermore, analyses of force distributions in Jamison *et al.*<sup>11</sup> show that the difference between the portion of the load assumed by a primary and secondary load-bearing motor will generally decrease with increasing motor compliance. Relaxation times for a compliant multiple motor complexes will therefore be slow since their motors will step at similar rates, which will reduce the rate that the average motor separation distance changes in time. Overall, these results show that multiple kinesin relaxation phenomena will be very sensitive to structural and mechanical parameters affecting a complex’s configuration-dependent free energies and how loads are distributed between its motors.

## CONCLUSIONS

The cooperative behaviors of coupled kinesin motor proteins were examined *via* the discrete-state stochastic approach. The ability of this method to account for the

majority of the relevant states occupied by a complex as well as the transitions between them, and its success in reproducing key experimental observations found with experimental analyses of structurally-defined kinesin complexes, provided a basis to explore how kinesin cooperation is influenced by the structural, mechanical and biochemical properties of a motor complex. Overall, the present results suggest that multiple kinesin force production and velocities will be relatively insensitive to the organization of motors on cargos, their stiffness and cargo size. Responses to these factors are found, yet they are generally small and do not influence the abilities of multiple kinesins to cooperate productively as a team. These predictions suggest that the net negative cooperative behaviors found in previous multiple kinesin studies are likely robust, and will apply to various transport scenarios where multiple kinesins are organized differently on different types of cargos. Yet, it is important to note that this may not be the case for other motor proteins. For example, recent experimental and theoretical studies on myosins V indicate that dynamic behavior of multiple myosins V depend stronger on elasticity and cargo sizes. Then collective dynamics of myosins V could be tuned by other cellular processes more precisely.<sup>10,20</sup> It will be interesting to test these ideas directly by studying other motor protein systems *via* advanced theoretical and experimental methods.

In contrast to structural and mechanical parameters, biochemical factors affecting motor-filament affinities are found to influence, appreciably, the extent to which kinesin systems will adopt state where the motors can share the applied load on a cargo. One main reason for this distinction stems from the fact that multiple kinesin complexes generally possess a broad range of states where only one motor in the complex bears the applied load, and hence the differences in the free energy between these states and single-motor bound states are negligible. Structural factors that alter load distributions within a complex tend not to affect the energies of these configurations. However, biochemical factors such as the unloaded free energy of kineins–microtubule association alter the energies of all motor-bound states. Furthermore, these factors affect the timescale that motors remain filament-bound, and hence, influence whether a complex has the opportunity to evolve its bound geometry from a single-motor-bound state to productive load-sharing states.

In contrast to cargo detachment forces and velocities, the relaxation dynamics is found to be very sensitive to structural, mechanical and chemical parameters. Thus, while dependent on a number of factors, these factors can influence whether a multiple kinesin system will achieve a steady-state in circumstance where loads change temporally, as will be the case during bidirectional

transport. If forces acting on motor proteins change rapidly, some forms of motors complexes might not have time to adopt their geometries to steady-state conditions, giving rise to hysteresis and other complicated effects that might confound interpretations. In other words, deviations from stationary-state behavior of motor proteins could significantly modify cooperative motors responses, and one should be careful in assessing competitions between motors and cannot necessarily assume that strong or weak motors would win a tug of war.

### ACKNOWLEDGMENTS

This work was supported by grants from the National Science Foundation (MCB-0643832), the National Institute of Health (1R01GM094489-01) and the Welch Foundation (C-1559 to A.B.K. and C-1625 to M.R.D.).

### REFERENCES

- <sup>1</sup>Alberts, B., *et al.* Molecular Biology of the Cell (4th ed.). USA: Taylor & Francis, 2002.
- <sup>2</sup>Ali, Y. M., G. G. Kennedy, D. Safer, K. M. Trybus, L. H. Sweeney, and D. M. Warshaw. Myosin Va and myosin VI coordinate their steps while engaged in an in vitro tug of war during cargo transport. *Proc. Natl. Acad. Sci. U.S.A.* 108:E535–E541, 2011.
- <sup>3</sup>Ali, Y. M., H. Lu, C. S. Bookwalter, D. M. Warshaw, and K. M. Trybus. Myosin V and Kinesin act as tethers to enhance each others' processivity. *Proc. Natl. Acad. Sci. U.S.A.* 105:4691–4696, 2008.
- <sup>4</sup>Ally, S., A. G. Larson, K. Barlan, S. E. Rice, and V. I. J. Gelfand. Opposite-polarity motors activate one another to trigger cargo transport in live cells. *Cell Biol.* 187:1071–1082, 2009.
- <sup>5</sup>Campas, O., Y. Kafri, K. B. Zeldovich, J. Casademunt, and J.-F. Joanny. Collective dynamics of interacting molecular motors. *Phys. Rev. Lett.* 97:038101, 2006.
- <sup>6</sup>Driver, J. W., K. D. Jamison, K. Uppulury, A. R. Rogers, A. B. Kolomeisky, and M. R. Diehl. Productive cooperation among processive motors depends inversely on their mechanochemical efficiency. *Biophys. J.* 101:386–395, 2011.
- <sup>7</sup>Driver, J. W., A. R. Rogers, K. D. Jamison, R. K. Das, A. B. Kolomeisky, and M. R. Diehl. Coupling between motor proteins determines dynamic behaviors of motor protein assemblies. *Phys. Chem. Chem. Phys.* 12:10398–10405, 2010.
- <sup>8</sup>Holzbaur, E. L. F., and Y. E. Goldman. Coordination of molecular motors: from in vitro assays to intracellular dynamics. *Curr. Opin. Cell Biol.* 22:4–13, 2010.
- <sup>9</sup>Howard, J. Mechanics of motor proteins and the cytoskeleton. Sunderland, MA: Sinauer Associates, 2001.
- <sup>10</sup>Jamison, K. D., J. W. Driver, and M. R. J. Diehl. Cooperative responses of multiple kinesins to variable and constant loads. *Biol. Chem.* 287:3357–3365, 2012.
- <sup>11</sup>Jamison, K. D., J. W. Driver, A. R. Rogers, P. E. Constantinou, and M. R. Diehl. Two kinesins transport cargo primarily via the action of one motor: implications for intracellular transport. *Biophys. J.* 99:2967–2977, 2010.
- <sup>12</sup>Klumpp, S., and R. Lipowsky. Cooperative cargo transport by several molecular motors. *Proc. Natl. Acad. Sci. U.S.A.* 102:17284–17289, 2005.
- <sup>13</sup>Kulić, I. M., A. E. X. Brown, H. Kim, C. Kural, B. Blehm, P. R. Selvin, P. C. Nelson, and V. I. Gelfand. The role of microtubule movement in bidirectional organelle transport. *Proc. Natl. Acad. Sci. U.S.A.* 105:10011–10016, 2008.
- <sup>14</sup>Kunwar, A., and A. Mogilner. Robust transport by multiple motors with nonlinear force-velocity relations and stochastic load sharing. *Phys. Biol.* 7:016012, 2010.
- <sup>15</sup>Kural, C., H. Kim, S. Syed, G. Goshima, V. I. Gelfand, and P. R. Selvin. Kinesin and dynein move a peroxisome in vivo: a tug-of-war or coordinated movement? *Science* 308:1469–1472, 2005.
- <sup>16</sup>Laib, J. A., J. A. Marin, R. A. Bloodgood, and W. H. Guilford. The reciprocal coordination and mechanics of molecular motors in living cells. *Proc. Natl. Acad. Sci. U.S.A.* 106:3190–3195, 2009.
- <sup>17</sup>Leduc, C., O. Campas, K. B. Zeldovich, A. Roux, P. Jolimaître, L. Bourel-Bonnet, B. Goud, J.-F. Joanny, P. Bassereau, and J. Prost. Cooperative extraction of membrane nanotubes by molecular motors. *Proc. Natl. Acad. Sci. U.S.A.* 101:17096–17101, 2004.
- <sup>18</sup>Leduc, C., N. Pavin, F. Julicher, and S. Diez. Collective behavior of antagonistically acting kinesin-1 motors. *Phys. Rev. Lett.* 105:128103, 2010.
- <sup>19</sup>Leduc, C., F. Ruhnnow, J. Howard, and S. Diez. Detection of fractional steps in cargo movement by the collective operation of kinesin-1 motors. *Proc. Natl. Acad. Sci. U.S.A.* 104:10847–10852, 2007.
- <sup>20</sup>Lu, H., A. K. Efremov, C. S. Bookwalter, E. B. Krementsova, J. W. Driver, K. M. Trybus, and M. R. Diehl. Collective dynamics of elastically coupled myosin V motors. *J. Biol. Chem.* 287(33):27753–27761, 2012.
- <sup>21</sup>Muller, M. J. I., S. Klumpp, and R. Lipowsky. Tug-of-war as a cooperative mechanism for bidirectional cargo transport by molecular motors. *Proc. Natl. Acad. Sci. U.S.A.* 105:4609–4614, 2008.
- <sup>22</sup>Ou, G. S., O. E. Blacque, J. J. Snow, M. R. Leroux, and J. M. Scholey. Functional coordination of intraflagellar transport motors. *Nature* 436:583–587, 2005.
- <sup>23</sup>Rogers, A. R., J. W. Driver, P. E. Constantinou, K. D. Jamison, and M. R. Diehl. Negative interference dominates collective transport of kinesin motors in the absence of load. *Phys. Chem. Chem. Phys.* 11:4882–4889, 2009.
- <sup>24</sup>Rogers, S. L., I. S. Tint, P. C. Fanapour, and V. I. Gelfand. Regulated bidirectional motility of melanophore pigment granules along microtubules in vitro. *Proc. Natl. Acad. Sci. U.S.A.* 94:3720–3725, 1997.
- <sup>25</sup>Ross, J. L., K. Wallace, H. Shuman, Y. E. Goldman, and E. L. F. Holzbaur. Processive bidirectional motion of dynein-dynactin complexes in vitro. *Nat. Cell Biol.* 8:562–570, 2006.
- <sup>26</sup>Uppulury, K., A. K. Efremov, J. W. Driver, D. K. Jamison, M. R. Diehl, and A. B. J. Kolomeisky. How the interplay between mechanical and nonmechanical interactions affects multiple kinesin dynamics. *Phys. Chem. B* 116:8846–8855, 2012.
- <sup>27</sup>Vale, R. D. The molecular motor toolbox for intracellular transport. *Cell* 112:467–480, 2003.
- <sup>28</sup>Xu, J., Z. Shu, S. J. King, and S. P. Gross. Tuning multiple motor travel via single motor velocity. *Traffic* 13:1198–1205, 2012.